

## *Supplementary Information*

### **Facet-dependent photo-Fenton degradation of *p*-arsanilic acid and arsenic redistribution on hematite**

Yuhan Guo<sup>a,b</sup>, Yixuan Song<sup>a</sup>, Shengrui Xu<sup>a</sup>, Zhenli Zhu<sup>a</sup>, Lei Ouyang<sup>a,b,c,\*</sup> and Qin Shuai<sup>a,\*</sup>

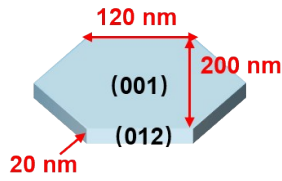
<sup>a</sup> State Key Laboratory of Geomicrobiology and Environmental Changes, Faculty of Materials Science and Chemistry, China University of Geosciences, Wuhan 430074, China.

<sup>b</sup> Hunan Provincial Key Laboratory of Geochemical Processes and Resource Environmental Effects, Geophysical and Geochemical Survey Institute of Hunan, Changsha 410114, China.

<sup>c</sup> Shenzhen Research Institute of China University of Geosciences, Shenzhen, 518063, China.

Fig. S1-S6 are included.

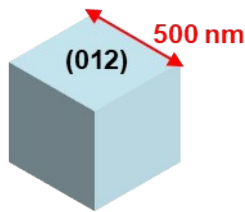
The surface area ratio of different facets in HNPs is calculated based on the regular hexagon shape and its geometric dimensions. The detail calculation formula is as follows:



$$\text{Ratio}(001) = \frac{2 \cdot S_{(001)}}{2 \cdot S_{(001)} + 6 \cdot S_{(012)}} = \frac{2 \cdot (100 \cdot \frac{100}{\sqrt{3}} \cdot 2 + 120 \cdot 200)}{2 \cdot (100 \cdot \frac{100}{\sqrt{3}} \cdot 2 + 120 \cdot 200) + 6 \cdot 20 \cdot 120} = 83.2\%;$$

$$\text{Ratio}(012) = \frac{6 \cdot S_{(012)}}{2 \cdot S_{(001)} + 6 \cdot S_{(012)}} = \frac{6 \cdot 20 \cdot 120}{2 \cdot (100 \cdot \frac{100}{\sqrt{3}} \cdot 2 + 120 \cdot 200) + 6 \cdot 20 \cdot 120} = 16.8\%.$$

For HNCs, the nanocubes are enclosed entirely by six crystallographic planes belonging to the {012} family. Thus, the proportion of {012} facets is 100%.



$$\text{Ratio}(012) = 100\%.$$

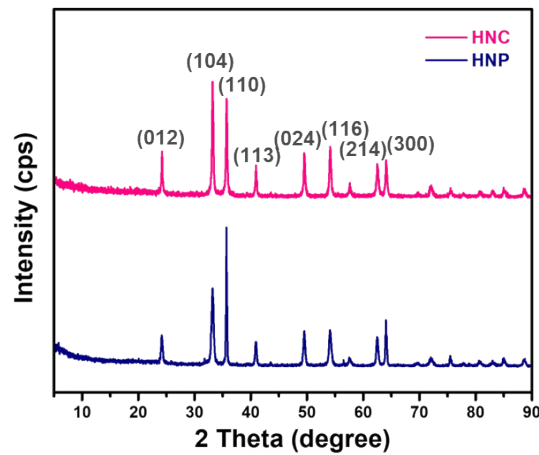


Fig. S1 XRD patterns of HNP and HNC.

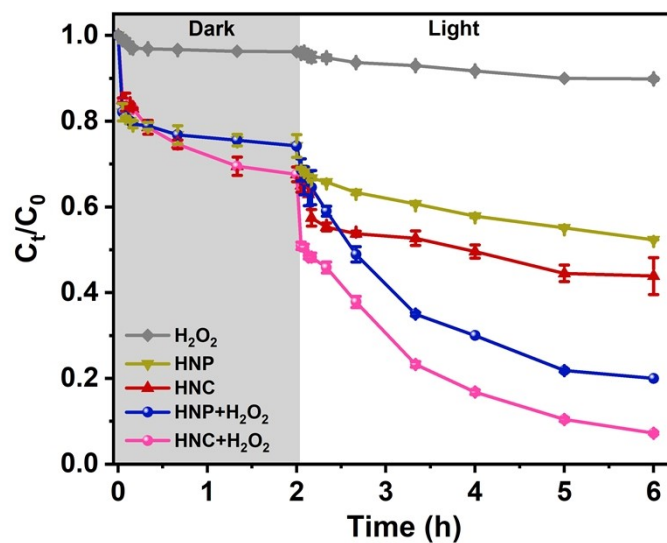


Fig. S2 Integrated performance of hematite in the dark adsorption and subsequent photocatalytic degradation of *p*-ASA.

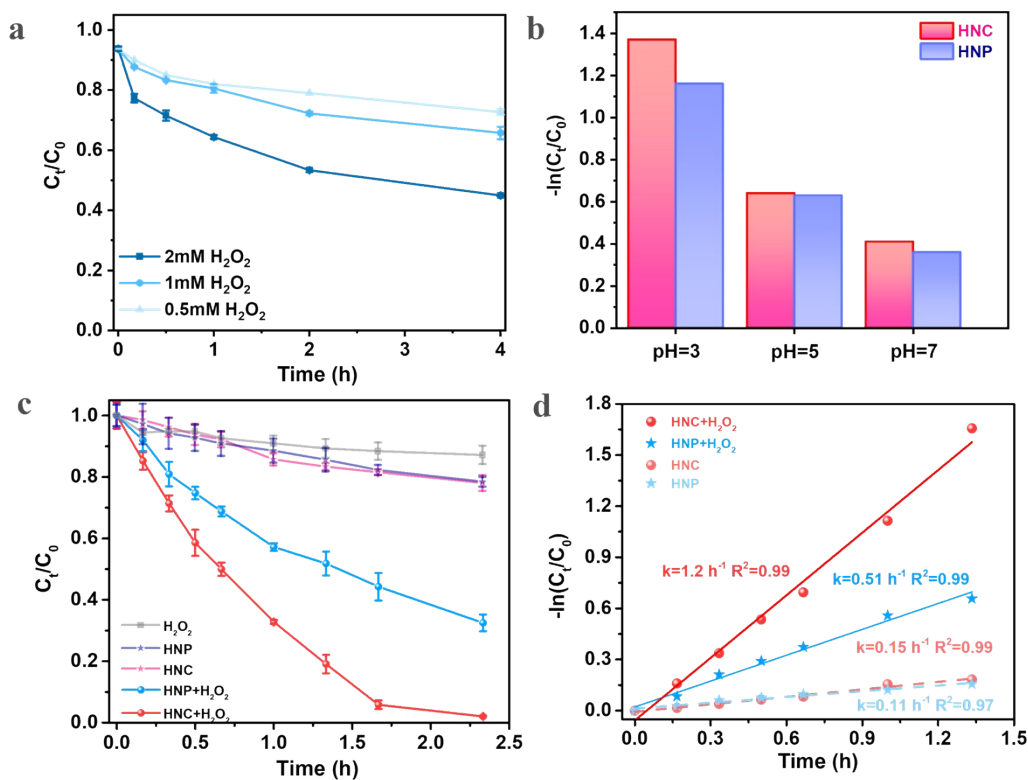


Fig. S3 Effects of reaction conditions on the photocatalytic degradation of *p*-ASA. (a) Degradation profiles at varying  $\text{H}_2\text{O}_2$  concentrations. (b) Comparison of the apparent rate constants ( $k$ ) under different pH conditions. (c) Temporal concentration change of *p*-ASA at pH=3. (d) Corresponding Langmuir-Hinshelwood pseudo-first-order kinetic fitting at pH=3.

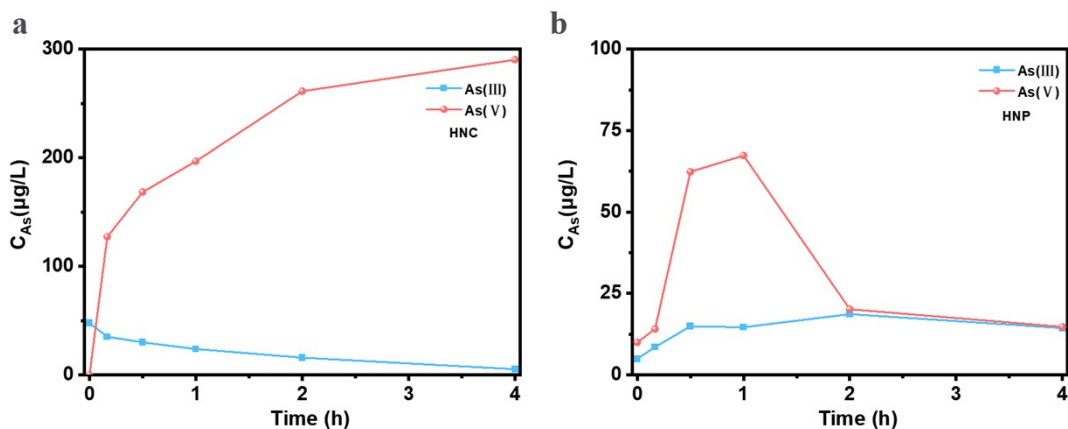


Fig. S4 Time-dependent concentrations of inorganic arsenic species ( $\text{As(III)}$  and  $\text{As(V)}$ ) released during the photocatalytic degradation of *p*-ASA.

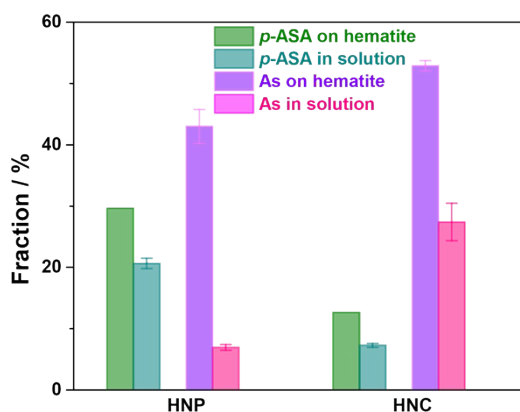


Fig. S5 Post-degradation distribution of arsenic species in the solid and liquid phases.

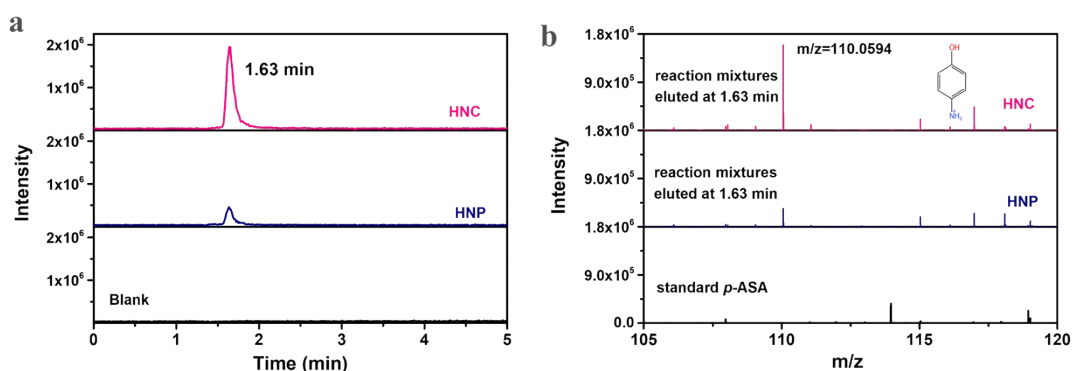


Fig. S6 Analysis of degradation intermediates. (a) HPLC-MS chromatogram of the reaction solution. (b) Mass spectrum of the intermediate eluting at 1.63 min, identified as *p*-aminophenol.